hep-ph/0207026

FERMILAB-Pub-02/129-T
DAMTP-2002-79
Cavendish-HEP-02/07
June 2002

Trilepton Events and $B_s \to \mu^+\mu^-$: No-lose for mSUGRA at the Tevatron?

A. Dedes[a], H. K. Dreiner[a], U. Nierste[b], and P. Richardson[c]

[a] *Physikalisches Institut der Universität Bonn, Nußallee 12, D-53115 Bonn, Germany*

[b] *Fermi National Accelerator Laboratory, Batavia, IL 60510-500, USA*[1]

[c] *Cavendish Laboratory and DAMTP, University of Cambridge, UK*

Abstract

We study the Tevatron search potential for minimal supergravity (mSUGRA) and find two observables which reveal complementary information on the mSUGRA parameter space: the "gold-plated" decays of charginos/neutralinos to trilepton final states and the rare decay $B_s \to \mu^+\mu^-$. For the universal gaugino mass, $M_{1/2}$ below 250 GeV and for the universal scalar fermion mass, M_0 outside of 200-370 GeV we face a "no-lose" situation for the Tevatron: If $\tan\beta \lesssim 30$, the Tevatron has a chance to see the trilepton events but not $B_s \to \mu^+\mu^-$ during Run IIa, whereas for larger $\tan\beta$ the trilepton events become invisible (at least with an integrated luminosity of 2 fb^{-1}) while $B_s \to \mu^+\mu^-$ is enhanced to an observable level. For this study we perform an updated analysis of the trilepton signature which includes the full set of the decay matrix elements and spin correlations. This leads to a new, more promising search reach for the Tevatron.

[1]Fermilab is operated by URA under DOE contract No. DE-AC02-76CH03000.

1 Introduction and Motivation

Even after imposing R-parity conservation by hand, the minimal supersymmetric standard model (MSSM) has an embarrassingly large number of parameters. The construction of a model with only a few parameters is desirable for æsthetic and practical reasons. The minimal supergravity (mSUGRA) scenario [1, 2] is currently the most elegant solution to this problem. In mSUGRA, local supersymmetry (supergravity) is spontaneously broken in the hidden-sector: the minimum of the scalar potential violates supersymmetry. The superpartner of the graviton, the spin 3/2 gravitino, acquires a mass, via this super-Higgs effect [3]. Supersymmetry breaking is communicated to the observable sector via gravity interactions. The quantum gravitational corrections are in principle non-renormalizable, but taking the "flat" limit where the Planck scale goes to infinity ($M_P = (8\pi G_N)^{-1/2} \to \infty$) we are left with an effective theory which is renormalizable. The most general form of the low energy *scalar potential* after supersymmetry breaking [2] contains the following free parameters:[2]

1. mass terms for the scalar particles, m_{ij},
2. trilinear couplings, h_{ijk},
3. the bilinear terms, b_{ij}.

These terms break supersymmetry softly in the sense that no quadratic divergences appear in the theory [4]. The number of parameters is dramatically reduced if the superpotential splits into a hidden-sector and a visible sector part [5]. Then these parameters are all universal

$$m_{ij} = M_0\,\delta_{ij}, \qquad h_{ijk} = A_0\,Y_{ijk}, \qquad b_{ij} = B_0\,\delta_{ij}. \tag{1}$$

B_0 and the magnitude of the superpotential Higgs mixing parameter μ are fixed by electroweak symmetry breaking [6]. Outside of the scalar sector, there is a further universal soft supersymmetry breaking parameter: the common gaugino mass, $M_{1/2}$. In the Higgs sector there is an additional parameter: $\tan\beta$, the ratio of the vacuum expectation values of the two neutral, CP-even Higgs fields. We thus have a total of 5 parameters in mSUGRA

$$M_0,\ A_0,\ M_{1/2},\ \mathrm{sgn}\,\mu,\ \tan\beta. \tag{2}$$

The parameters M_0, A_0, $M_{1/2}$, are expected to be universal at the *Planck scale*, where supersymmetry breaking is mediated from the hidden-sector to the observable sector. In order to obtain weak-scale predictions we must use the renormalization group equations (RGEs) to evolve the parameters from M_P down to M_W. In addition, there could be unification at the grand unified (GUT) scale $M_X = \mathcal{O}(10^{16}\,GeV)$ in an unknown simple group such as $SU(5)$ or $SO(10)$. This would strongly modify the RGEs between the Planck scale and the GUT scale. In order to avoid this model dependence, we consider M_0, A_0, $M_{1/2}$, to be universal at the GUT scale. We thus neglect any effects of the running

[2] If R-parity is conserved there is only one bilinear parameter $b_{ij} = b$.

of the RGEs between M_P and M_X. In our numerical analysis, $\tan\beta$ and $\mathrm{sgn}\,\mu$ are fixed at the weak scale.

The mSUGRA model with universal parameters is a simple, well motivated model for the low-energy supersymmetric spectrum. If an observable in this model deviates substantially from the standard model (SM), then we would expect to find a similar deviation in a more general non-universal case, modulo accidental cancellations. Thus we expect to be able to obtain more general results already in this simplified model. However, correlations between observables in mSUGRA such as $B_s \to \mu^+\mu^-$ versus $(g-2)_\mu$ [7] are typically lost in the more general case due to the additional parameter freedom.

After more than 25 years there is still no experimental evidence for supersymmetry (SUSY). In principle we expect two kinds of signatures: 1) an indirect signature via a deviation from a SM prediction or 2) a direct detection of a supersymmetric particle. It is the purpose of this letter to demonstrate the complementarity of these two approaches in two specific examples. For the direct search we consider the trilepton signature, which was first proposed in the context of supersymmetry in [8–11], and has since become a standard search mode for supersymmetry production. We wish to investigate the correlation of this signature in mSUGRA with the rare B_s meson decay $B_s \to \mu^+\mu^-$. We expect these two signatures to be observable at Run II of the Tevatron.

In the following we present the actual status of leptonic B meson decays. We then proceed and perform a brand new analysis of the multilepton signatures in mSUGRA. We confirm the results of Matchev and Pierce [12, 13]. We then go beyond this work to include the full matrix elements for the supersymmetric decays, which were not included in ISASUSY at the time. This leads to a more promising discovery reach for Run II of the Tevatron.

2 The decay $B_s \to \mu^+\mu^-$

In the SM, the leptonic decays $B_{s,d} \to \ell^+\ell^-$ are dominated by Z-boson penguin and box diagrams involving top quark exchange. The decay amplitude is helicity suppressed and thereby proportional to the lepton mass. The resulting small branching ratios are well below the upper bounds set by past and present experiments; the current situation is summarized in Table 1. The uncertainty in the SM predictions [14] of Table 1 mainly stems from the decay constants $f_{B_d} = (200 \pm 30)$ MeV and $f_{B_s} = (230 \pm 30)$ MeV [15]. While the element $|V_{ts}| = 0.040 \pm 0.002$ of the Cabibbo-Kobayashi-Maskawa (CKM) matrix entering the B_s decays is well-known from CKM unitarity, the B_s decays suffer from an additional uncertainty due to $|V_{td}|$. From a global fit to the unitarity triangle one finds $0.15 \le |V_{td}/V_{ts}| \le 0.23$ [16]. We use the $\overline{\mathrm{MS}}$ b-quark mass $m_b(m_b) = 4.25$ GeV and assume a fixed[3] $\overline{\mathrm{MS}}$ value for the top quark mass, $m_t(m_t) = 167$ GeV. This corresponds to a pole mass of $m_t = 175$ GeV. There is an additional small uncertainty of $\pm 0.3 \times 10^{-9}$

[3] In the mSUGRA analysis below, $m_t(m_t)$ is not fixed due to the variation of the strong coupling constant α_s with the SUSY spectrum under the assumption of gauge coupling unification. However, the effect of this variation is small compared to the hadronic uncertainty.

Channel	Expt.	Bound (90% CL)	SM prediction [14]
$B_s \to e^+e^-$	L3 [17]	$< 5.4 \times 10^{-5}$	$(8.9 \pm 2.3) \times 10^{-14}$
$B_s \to \mu^+\mu^-$	CDF [18]	$< 2.0 \times 10^{-6}$	$(3.8 \pm 1.0) \times 10^{-9}$
$B_s \to \tau^+\tau^-$	LEP [19]	< 0.05	$(8.2 \pm 2.1) \times 10^{-7}$
$B_d \to e^+e^-$	CLEO [20]	$< 8.3 \times 10^{-7}$	$(2.4 \pm 0.7 \pm 0.7) \times 10^{-15}$
$B_d \to \mu^+\mu^-$	CLEO [20]	$< 6.1 \times 10^{-7}$	$(1.0 \pm 0.3 \pm 0.3) \times 10^{-10}$
$B_d \to \tau^+\tau^-$	LEP [19]	< 0.015	$(2.1 \pm 0.6 \pm 0.6) \times 10^{-8}$

Table 1: *The experimental status and the SM predictions for the branching ratios* $\mathcal{B}(B_{s,d} \to \ell^+\ell^-)$*. The error in the* B_s *branching ratios mainly originates from the uncertainty in* f_{B_s}*, the two errors in the* B_d *branching ratios correspond to the uncertainties in* f_{B_d} *and* $|V_{td}|$*.*

in $\mathcal{B}(B_s \to \mu^+\mu^-)$ when scanning the top mass in its experimental range. Since we are interested in order-of-magnitude effects from supersymmetry, we can safely neglect the hadronic uncertainty and work with the central values of the decay constants and CKM elements.

As $\mathcal{B}(B \to \ell^+\ell^-) \propto m_\ell^2$, the branching ratio is largest for $\ell = \tau$. Yet τ-lepton searches are very difficult at hadron colliders. Therefore the best mode to search for new physics is $B_s \to \mu^+\mu^-$. Still the decay to $\tau^+\tau^-$ has a very weak bound and we believe that an analysis of the existing LEP data could result in a stronger bound. Leptonic branching ratios of B_d mesons are smaller by a factor of $|V_{td}/V_{ts}|^2 \lesssim 0.05$ than the leptonic decays of B_s mesons. From Table 1 we see that CLEO [20] has provided strong bounds for the electron and muon final states. Again, a dedicated search for the final state τ's remains to be performed. The BaBar and Belle experiments could improve on Table 1 as well.

From now on we restrict ourselves to the decay mode $B_s \to \mu^+\mu^-$. In the SM, the decay mode $B_s \to \mu^+\mu^-$ is experimentally challenging due to its small branching ratio. However, it has a quite distinctive and unique signature. During Run I of the Tevatron the CDF experiment has set an upper bound at 95% CL. [18]

$$\mathcal{B}(B_s \to \mu^+\mu^-) < 2.6 \times 10^{-6}\,, \tag{3}$$

based on an analysis using very tight cuts to achieve an essentially background-free framework. When extrapolated to Run IIa, which corresponds to an integrated luminosity of 2 fb^{-1}, this method yields a single event sensitivity of $\mathcal{B}(B_s \to \mu^+\mu^-) = 1.0 \cdot 10^{-8}$ [21]. A recent analysis [22] found that CDF can discover $B_s \to \mu^+\mu^-$ in Run IIb with an integrated luminosity of 15 fb^{-1}, if $\mathcal{B}(B_s \to \mu^+\mu^-) > 1.2 \times 10^{-8}$. Currently further sophisticated studies are underway, and better cuts may well improve the explorable range of $\mathcal{B}(B_s \to \mu^+\mu^-)$. The SM range will certainly be accessible to the LHC experiments [23].

The helicity suppression gives the leptonic B decays a very special rôle in the search for new physics, because they are sensitive to new chirality-flipping interactions like extended Higgs sectors with enhanced Yukawa couplings. This scenario occurs in the two-Higgs-doublet model (2HDM) and the MSSM, if $\tan\beta$ is large. In particular no other observable in B physics is more sensitive to effects from non-standard neutral Higgs bosons than

$\mathcal{B}(B \to \ell^+\ell^-)$. In the type-II 2HDM the extra contribution to the decay amplitude grows like $\tan^2\beta$ and is roughly of the same size as the SM amplitude [24, 25]. In the MSSM, however, the amplitude involves three powers of $\tan\beta$, so that

$$\mathcal{B}(B_s \to \mu^+\mu^-) \propto \tan^6\beta. \tag{4}$$

This leads to an enhancement over the SM value by up to three orders of magnitude. This holds even in the flavour-universal MSSM, where flavour changes occur in weak vertices only and come with the usual CKM elements [25–27]. Moreover, in the limit of infinite SUSY mass parameters the MSSM contribution does not vanish, because the MSSM approaches a general 2HDM with flavour-changing neutral Higgs couplings in this limit. This feature and the resulting importance of B physics to probe the large $\tan\beta$ regime of the MSSM was first emphasized in [28]. The supersymmetric contributions enhancing $\mathcal{B}(B_s \to \mu^+\mu^-)$ will also affect the branching ratio and forward-backward asymmetry in the decay

$$B \to (\pi, K)\ell^+\ell^-, \tag{5}$$

but these effects are small and strongly correlated with $\mathcal{B}(B_s \to \mu^+\mu^-)$ and will only be measurable, if $\mathcal{B}(B_s \to \mu^+\mu^-)$ is close to its experimental upper bound [27, 29].

The first analysis of $B_s \to \mu^+\mu^-$ in the minimal supergravity scenario (mSUGRA) revealed an interesting correlation of $\mathcal{B}(B_s \to \mu^+\mu^-)$ with the muon anomalous magnetic moment $(g-2)_\mu$ and the mass of the lightest Higgs boson [7]: If $(g-2)_\mu$ exceeds the SM prediction by 40×10^{-10} (which is the maximum allowed from BNL [30,31]), $\mathcal{B}(B_s \to \mu^+\mu^-)$ is larger by a factor of 10–100 than in the SM and within reach of Run II of the Tevatron. If the decay $B_s \to \mu^+\mu^-$ is observed at Run II of the Tevatron, then in mSUGRA the mass of the lightest neutral CP-even Higgs boson should be less than 120 GeV. The results of Ref. [7] were recently confirmed in Ref. [22], where also constraints from dark matter were included. A nice observation was made in Ref. [32]: alternative SUSY breaking scenarios imprint signatures on $(g-2)_\mu$ and $\mathcal{B}(B_s \to \mu^+\mu^-)$ which are very different from those found for mSUGRA in Ref. [7]. A substantial enhancement of $\mathcal{B}(B_s \to \mu^+\mu^-)$ in anomaly-mediated SUSY breaking scenarios is impossible and also hard to accommodate with gauge-mediated SUSY-breaking. Thus an observation of $B_s \to \mu^+\mu^-$ at Run II of the Tevatron can be viewed as a signature of supersymmetry with gravity-mediated supersymmetry breaking. In our numerical analysis of $\mathcal{B}(B_s \to \mu^+\mu^-)$ we use the formulae of [27] supplemented with an all-order resummation of $\tan\beta$-enhanced supersymmetric QCD corrections [33]. Other QCD corrections (neglecting gluino contributions) were calculated in [34] and found to be small, if the renormalization scale is chosen close to the masses of the SUSY particles propagating in the loop.

3 Multilepton SUSY events

Trileptons are an old phenomenological signature of cascade decays in particle physics [35, 36]. They were first applied in supersymmetry in the cascade decays of electroweak

gauge bosons via light gauginos [8].[4] A first systematic study was performed in [9–11]. It was first shown in [38] that off-shell W, Z cascade decays via gauginos can also lead to promising trilepton signatures. The study was however restricted to $\tan\beta = 1$. Also the sparticle spectrum was not computed in terms of a small set of MSSM parameters. These points were generalized in [39]. An extension of the Tevatron studies to the LHC was performed in [40][5] and to a $\sqrt{s} = 4\,\text{TeV}$ Tevatron in [42]. A first study for the high-luminosity Run II at the Tevatron was performed in [43, 44]. A first study of what we now call mSUGRA was performed in [45] including a multichannel analysis. Various unification scenarios were probed via the trilepton signature in [46, 47]. In [48, 49] the case of large $\tan\beta$ was first considered. This can lead to additional contribution of τ leptons in the final state which was discussed in detail in [50–54]. An update improving many features of the analysis has recently been performed in [12, 55] including a reevaluation of the $W\gamma^*$ background [13]. We now discuss in detail how we have improved on this work.

3.1 Numerical Analysis

In general our strategy for the analysis of the multilepton signatures closely follows that of Matchev and Pierce [12, 13]. The major differences between these studies are:

- While Matchev and Pierce [12, 13] used leading-order (in QCD) cross sections for both the signal and background processes we use next-to-leading order calculations for the background and most important signal processes.

- In Refs. [12,13] the authors used ISAJET 7.42 [56] for the simulation of the signal. For the background they used PYTHIA 6.115 [57]. In Ref. [13] they used a combination of PYTHIA and COMHEP [58] for the WZ background.[6] Instead, we use HERWIG6.4 [59] to simulate the signal and a combination of HERWIG and COMPHEP to simulate the background. This has a number of advantages due to recent improvements in HERWIG. While ISAJET7.42 uses matrix elements for the three body decays of the gauginos it performs the production and decay of the SUSY particles independently. HERWIG6.4 makes use of the method described in [60] to perform the SUSY decays including all the momentum and spin correlations. One of the major advantages of our studies is that the spin correlation algorithm used in HERWIG can use the TAUOLA decay package [61] to give the correct helicity of the tau on an event-by-event basis, rather than averaging as was done in [12, 13]. ISAJET7.58 is used to calculate the SUSY spectrum and decay rates.

In our simulation we make use of the PGS [62] detector simulation. This is a more recent version of the SHW package. The default PGS parameters are used together with the following additions.

[4] Implicitly these signatures appear in Ref. [37].

[5] For analogous signatures for gluino production see for example [41].

[6] This brief summary is based on a private communication with Konstantin Matchev and differs slightly from the presentation in the papers.

1. A requirement that the total transverse energy in a cone of size $\Delta R = \sqrt{\Delta\phi^2 + \Delta\eta^2} = 0.4$ about the direction of a muon is less than 2 GeV. Here ϕ is the azimuthal angle of the particle, $\eta = -\ln\tan(\theta/2)$ is the pseudo-rapidity, and θ is the angle of the particle with respect to the incoming beam.

2. The missing transverse energy, $\not\!\!E_T$, which is calculated in PGS using the calorimeter cells, is corrected to include any muons. The transverse energy $E_T = E\sin\theta$, where E is the energy of a particle.

3. A cut on the ratio of the electromagnetic, $E_{\rm em}$, to hadronic energy, $E_{\rm had}$, in a jet $E_{\rm em}/E_{\rm had} < 10$ to avoid electrons being considered as jets.

These modifications are virtually identical[7] to those made in Ref. [13].

3.2 Background and Signal

The major backgrounds to multilepton production are:

WW: Here the background is from the production of leptons in the cascade decay of the W bosons. These events are simulated using HERWIG6.4 and the results normalized to the next-to-leading order result from MCFM [63].

WZ: In this case the leptons come from the decay of the gauge bosons. This is the main physics background in most of the channels. As this channel is so important, rather than use HERWIG, which does not include all the diagrams, we use COMPHEP to generate all the Feynman diagrams for the four-fermion final state. HERWIG is then used to generate the initial-state radiation and hadronization of the partonic events generated with COMPHEP. The results are normalized to the next-to-leading order cross section calculated using MCFM [63].

ZZ: The background comes from the production of leptons in the decay of the Z bosons. These events are simulated using HERWIG6.4 with a next-to-leading order normalization from MCFM [63].

W+jets: In these events the background comes from one real lepton produced in the decay of the W and additional fake leptons from the mis-identification of isolated hadrons as leptons. The simulation of isolated hadrons producing fake electrons and muons cannot be performed reliably using Monte Carlo event generators and therefore we adopt the same procedure as in Ref. [13] in order to estimate this rate from the Run I CDF data. The SHW simulation, which was the predecessor to PGS, gives a reasonable simulation of fake tau production [13, 64], and we therefore rely on the Monte Carlo simulation for fake tau production. HERWIG6.4, which includes the matrix-element correction to the parton shower as described in Ref. [65], is used to

[7] In Ref. [13] the tracking coverage is extended from $|\eta| \leq 1.5$ to $|\eta| \leq 2.0$ however this is now the default in PGS.

simulate this background. The results of the Monte Carlo simulation are re-scaled to the next-to-leading-order cross section calculated using MCFM [66].

Z+jets: In this case the background comes from either the leptons produced in the cascade decay of the Z, with additional fake leptons as described above, charge misidentification, or leptons from the Z itself depending on the channel. Again HERWIG6.4 which includes the matrix-element correction to the initial-state radiation is used to simulate this process. As with the W+jets background, the results of the simulation are normalized using the next-to-leading-order cross section calculated with MCFM [66]. The fake lepton rate is calculated as for the W+jets events.

$t\bar{t}$: The background comes from the semi-leptonic decay of the top quarks. We simulate this background using HERWIG6.4 and use the next-to-leading-order with next-to-leading-log resummation calculation of Ref. [67] to normalize the results.

There is also a potential background from the production of $b\bar{b}$ followed by the semi-leptonic decay of the produced b-flavoured hadrons. However, this should be negligible after the isolation and cuts on the transverse momentum, p_T, of the leptons.

In all cases we use HERWIG6.4 to simulate the signal. The cross sections for $\tilde{\chi}_2^0\tilde{\chi}_1^\pm$ and $\tilde{\chi}_1^+\tilde{\chi}_1^-$, which give the dominant contribution to the SUSY production, are normalized to the next-to-leading order cross section using the results of [68]. The leading-order cross section from HERWIG is used for the remaining processes.

3.3 Cuts

The basic idea of the analysis is to take several different cuts, which should differentiate between the signal and the background, consider all possible combinations of the cuts at each point in parameter space and optimize the choice of cuts in order to maximize $S/\sqrt{B}$, where S and B are the number of signal and background events respectively. In addition to the requirement of $S/\sqrt{B} > 5$ all the contours shown also require that there at least five signal events.

The cuts can be split into two types: channel-independent cuts and those which are specific to a given channel.

The channel independent cuts we use are:

1. Five possible cuts on the missing transverse energy, $\not{E}_T > \{15, 20, 25, 30\}$ GeV or no cut;

2. An optional veto on the presence of QCD jets with $E_T > \{10, 15, 20, 25, 30\}$ GeV in the event.

3. A cut on the minimum invariant mass of any opposite sign same flavour electron or muon (OSSF) pairs in the event $m_{\ell\ell} > \{5, 10, 15, 20, 25, 30, 35, 40, 45, 50, 55, 60\}$ GeV, or no cut.

4. A cut on the maximum invariant mass of any OSSF pairs in the event $m_{\ell\ell} < \{50, 60, 70, 80\}$ GeV, or a cut on the minimum difference between the mass of any OSSF pair and the Z mass $|M_{\rm Z} - m_{\ell\ell}| > \{10, 15\}$ GeV, or no cut.

5. A cut removing any events which have an electron or muon with transverse mass $65\,{\rm GeV} \leq {\rm m_T} \leq 85\,{\rm GeV}$. The transverse mass is given by $m_T^2 = 2|p_{T\ell}||p_{T\rm miss}|(1 - \cos\Delta\phi)$, where $p_{T\ell}$ is the transverse momentum of the lepton, $p_{T\rm miss}$ is the missing transverse momentum and $\Delta\phi$ is the azimuthal angle between the lepton and the missing transverse momentum.

The channel dependent cuts are:

1. For the trilepton and like-sign lepton signature we require a central electron or muon with $|\eta| \leq 1$ and $p_T > 11, 15, 20$ GeV, or no requirement for a central lepton.

2. For the lepton+ tau jet channel we require that the tau decay only has one prong[8] and that the fraction of the tau jet's momentum carried by the charged track is greater than 80%, as suggested in [69].

3. A cut on the transverse momenta of the leptons is also applied depending on the channel, the cuts for the various different channels are given in Table 2.

These cuts are the same as used in Ref. [12, 13] *apart* from one extra missing transverse energy cut and the cut on the momentum of the track in the tau jets.

4 Discussion

4.1 Trilepton (3L) Channel

We first discuss the trilepton (3L) channel. The production cross section for the chargino-neutralino pair, $\tilde{\chi}_1^{\pm}\tilde{\chi}_2^{0}$, scales like $M_{1/2}^{-11/2}$ and is thus only relevant in regions with small $M_{1/2}$, *i.e.* $M_{1/2} \lesssim 300$ GeV. We present our results in Fig. 1 on the $M_0 - M_{1/2}$ plane, for two different values of $\tan\beta$: 5 and 50. Starting with the (3L) events in the small $\tan\beta$ plot, we observe that the Tevatron could reach a 5σ discovery depending on its luminosity in the regions

$$\text{Region I } (3L, \tan\beta = 5) \;:\; \begin{cases} M_0 \lesssim 175 \text{ GeV} \;,\; M_{1/2} \lesssim 230 \text{ GeV} \;,\; \mathcal{L} = 2fb^{-1}\,, \\ M_0 \lesssim 190 \text{ GeV} \;,\; M_{1/2} \lesssim 270 \text{ GeV} \;,\; \mathcal{L} = 10fb^{-1}\,, \\ M_0 \lesssim 200 \text{ GeV} \;,\; M_{1/2} \lesssim 290 \text{ GeV} \;,\; \mathcal{L} = 30fb^{-1}\,, \end{cases}$$

$$\text{Region II } (3L, \tan\beta = 5) \;:\; \begin{cases} M_0 \gtrsim 480 \text{ GeV} \;,\; M_{1/2} \lesssim 190 \text{ GeV} \;,\; \mathcal{L} = 10fb^{-1}\,, \\ M_0 \gtrsim 360 \text{ GeV} \;,\; M_{1/2} \lesssim 220 \text{ GeV} \;,\; \mathcal{L} = 30fb^{-1}\,, \end{cases}$$

[8] *i.e.* the tau jet only had one charged track.

Trilepton channel			
Cut Set	$p_T(\ell_1)$	$p_T(\ell_2)$	$p_T(\ell_3)$
1	11	5	5
2	11	7	5
3	11	7	7
4	11	11	11
5	20	15	10
Like-sign dilepton channel			
Cut Set	$p_T(\ell_1)$	$p_T(\ell_2)$	
1	11	9	
2	11	11	
3	13	13	
4	15	15	
5	20	20	
Dilepton+hadronic tau channel			
Cut Set	$p_T(\ell_1)$	$p_T(\ell_2)$	$p_T(\tau)$
1	8	5	10
2	8	5	15
3	11	5	10
4	11	5	15
5	15	10	15

Table 2: *Lepton p_T cuts, all the cuts are given in GeV.*

Region I is larger than in Ref. [12, 13] due to the extra missing transverse energy cut we have made. Region II is larger than in [12, 13] due to the lighter spectrum produced by ISAJET7.58 which gives a larger signal cross section than for the same SUGRA point with ISAJET7.42. Overall, we thus obtain a more promising trilepton search reach at Run II of the Tevatron than in previous studies. This is one of the main conclusions of this paper.

Although we present our analysis in terms of the fundamental parameters of mSUGRA $M_0, M_{1/2}, \tan\beta$, there exist mass sum rules [70] relating these parameters to the physical masses. We can thus approximately translate the mSUGRA parameters into the physical masses (up to a 10% accuracy),

$$\begin{aligned} 2m_{\tilde{\chi}_1^0} &\simeq m_{\tilde{\chi}_2^0} \simeq m_{\tilde{\chi}_1^\pm} \simeq \frac{1}{3} m_{\tilde{g}} \simeq 0.8 M_{1/2} \ , \\ m_{\tilde{q}} &\simeq \sqrt{M_0^2 + 4M_{1/2}^2} \ , \end{aligned} \tag{6}$$

where $m_{\tilde{\chi}_i^0}$ are the neutralino masses with the lightest being the LSP. $m_{\tilde{\chi}_i^\pm}$ denote the chargino masses. $m_{\tilde{g}}$ and $m_{\tilde{q}}$ denote the gluino and the heavy first and second generation squark masses, respectively. Thus the Tevatron trilepton reach is relevant for a lightest chargino and a next-to-lightest neutralino mass below 200 GeV and (indirectly) for a gluino mass below 600 GeV.

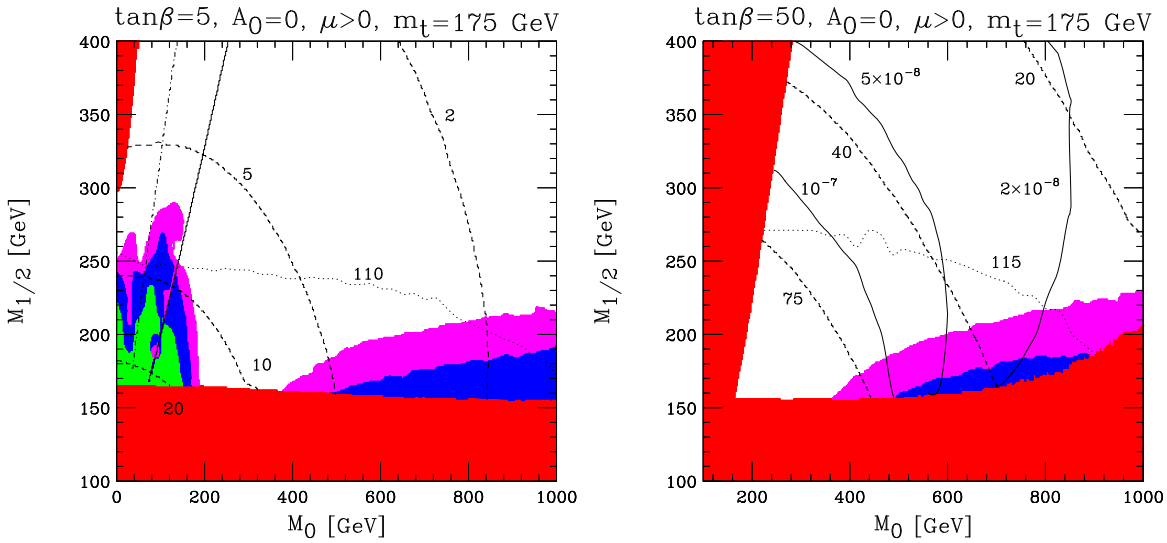

Figure 1: *Tevatron 5σ reach in the trilepton (3L) channel in the $M_0 - M_{1/2}$ plane in the mSUGRA scenario for small* $\tan\beta = 5$ *(left) and large* $\tan\beta = 50$ *(right) and $A_0 = 0$, $\mu > 0$ and $m_t = 175$ GeV. The shaded areas indicate the 5σ reach for an integrated luminosity of $30fb^{-1}$ (magenta), $10fb^{-1}$ (blue) and $2fb^{-1}$ (green) and from top to bottom, respectively. Dashed contours represent the SUSY contribution to the muon anomalous magnetic moment (in units of* 10^{-10}*) and the dotted contours are iso-mass contours of the lightest neutral Higgs boson. The solid contour (only for* $\tan\beta = 50$*) indicates the prediction for the branching ratio $\mathcal{B}(B_s \to \mu^+\mu^-)$. In the left (*$\tan\beta = 5$*) plot the solid line indicates where $m_{\tilde{\chi}_1^\pm} = m_{\tilde{\tau}_1}$ and the dot-dashed line $m_{\tilde{\chi}_1^\pm} = m_{\tilde{\nu}_\tau}$. The large red regions are excluded by theory and experiment [7].*

In Fig. 1 we include Higgs boson mass isocurvatures. The calculation of the light Higgs boson mass strictly follows the procedure described in Ref. [71]. In Region I the light Higgs boson mass varies from $(106 \div 112) \pm 3$ GeV where the error denotes a theoretical error in the calculation [72]. The current status for the Higgs boson mass bound from LEP is [73] : $M_h \gtrsim 113.5$ GeV for $\sin^2(\beta - \alpha) \simeq 1$, where α is the mixing angle in the CP-even Higgs sector. Thus $\tan\beta = 5$ has to be considered as the minimum $\tan\beta$ value where trilepton events can appear at the Tevatron since lower values will be in conflict with the LEP Higgs bound. The Higgs mass increases with $\tan\beta$.

For small values of $\tan\beta$ the supersymmetric contribution to the muon anomalous magnetic moment ($\delta a_\mu^{\rm SUSY}$) is in general small [74]. However, observing a trilepton signal in Region I will imply an at least moderate enhancement of a_μ by

$$\delta a_\mu^{\rm SUSY} \gtrsim 7 \times 10^{-10} \,, \tag{7}$$

due to the light charginos and sneutrinos. This is not the case in Region II, where $\delta a_\mu^{\rm SUSY}$ approaches zero.

There is a "null" $M_0 - M_{1/2}$ region at the Tevatron where no (3L) signal can be observed. This "null" region spans the parameter space where $200 \lesssim M_0 \lesssim 370$ GeV and is due to

the fact that off-shell, slepton mediated decays of the gauginos destructively interfere with the gauge boson mediated decays. Since the decay $B_s \to \mu^+\mu^-$ cannot be seen for such small values of $\tan\beta$ the "null" area has to be covered by other Tevatron searches (possibly Higgs searches [75]).

In Region II, a 5σ signal reach can be achieved with $\mathcal{L} = 10, 30\,\text{fb}^{-1}$. The light Higgs boson mass varies between $(106 \div 111) \pm 3$ GeV and the supersymmetric contributions to the muon anomalous magnetic moment are small,

$$\delta a_\mu^{\rm SUSY} \lesssim 5 \times 10^{-10}. \tag{8}$$

The CLEO/Belle/ALEPH allowed band for the branching ratio $\mathcal{B}(b \to s\gamma)$ does not set any constraint in the low $\tan\beta = 5$ region. In what follows, we adopt the conservative value[9] $2 \times 10^{-4} \lesssim \mathcal{B}(b \to s\gamma) \lesssim 5 \times 10^{-4}$.

We now turn to the discussion of the large $\tan\beta = 50$ plot in Fig. 1. The new Region I (low M_0) is not there any more (see below). The new Region II is given by

$$\text{Region II } (3L, \tan\beta = 50) \;:\; \begin{cases} M_0 \gtrsim 480 \text{ GeV} \;\;,\;\; M_{1/2} \lesssim 185 \text{ GeV} \;\;,\;\; \mathcal{L} = 10 fb^{-1}\,, \\ M_0 \gtrsim 360 \text{ GeV} \;\;,\;\; M_{1/2} \lesssim 230 \text{ GeV} \;\;,\;\; \mathcal{L} = 30 fb^{-1}\,. \end{cases}$$

The trilepton search only covers a small range of the $M_0 - M_{1/2}$ plane. There is a further strong constraint. The light Higgs boson mass varies in the range $(110 \div 119) \pm 3$ GeV from bottom to top where the contour $m_h = 115$ GeV is indicated in Fig. 1 as a dotted line. The LEP preliminary bound, $m_h \gtrsim 113$ GeV, is evaded (almost) everywhere in this plot. However, this is not true for the $b \to s\gamma$ constraint. Using the results in Ref. [76] we find that the excluded region due to the $b \to s\gamma$ constraint (accidentally) coïncides almost exactly with the area below the $m_h = 115$ GeV Higgs mass contour. We thus do not redraw it. This leaves only a small area for the 3L events to appear at the Tevatron

$$\text{Region II}' \; (3L, \tan\beta = 50) \;:\; M_0 \gtrsim 800 \text{ GeV}\,;\;\; M_{1/2} \sim 190 \div 230 \text{ GeV},\;\; \mathcal{L} = 30 fb^{-1}\,.$$

Notice also that this area is bounded for large M_0 due to the radiative electroweak symmetry breaking requirement.

By contrast, the decay mode $B_s \to \mu^+\mu^-$ is very promising for $\tan\beta = 50$. The branching ratio varies from a handful of events for large M_0 up to 100 events for low M_0 already with $\mathcal{L} = 2 fb^{-1}$. This very nicely complements the trilepton search and is the second main result of our paper: the tri-lepton search covers most of the low $\tan\beta$ region, the branching ratio $\mathcal{B}(B_s \to \mu^+\mu^-)$ covers most of the high $\tan\beta$ region.

Fig.1 also verifies what had been seen in Ref. [7]: the branching $\mathcal{B}(B_s \to \mu^+\mu^-)$ and the anomalous magnetic moment of the muon, $\delta a_\mu^{\rm SUSY}$, go hand-in-hand, *i.e.* there is a strong correlation. New experimental results for the anomalous magnetic moment of the muon are expected to appear as this manuscript is written. The up-to-date BNL excess is $-4.2 \times 10^{-10} \lesssim \delta a_\mu^{\rm SUSY} \lesssim 41.3 \times 10^{-10}$, at 90% C.L [30,31] with the central value $\delta a_\mu^{\rm SUSY} = 18 \times 10^{-10}$ [31].

[9] We follow here the discussion in the footnote no. 18 of Ref. [76].

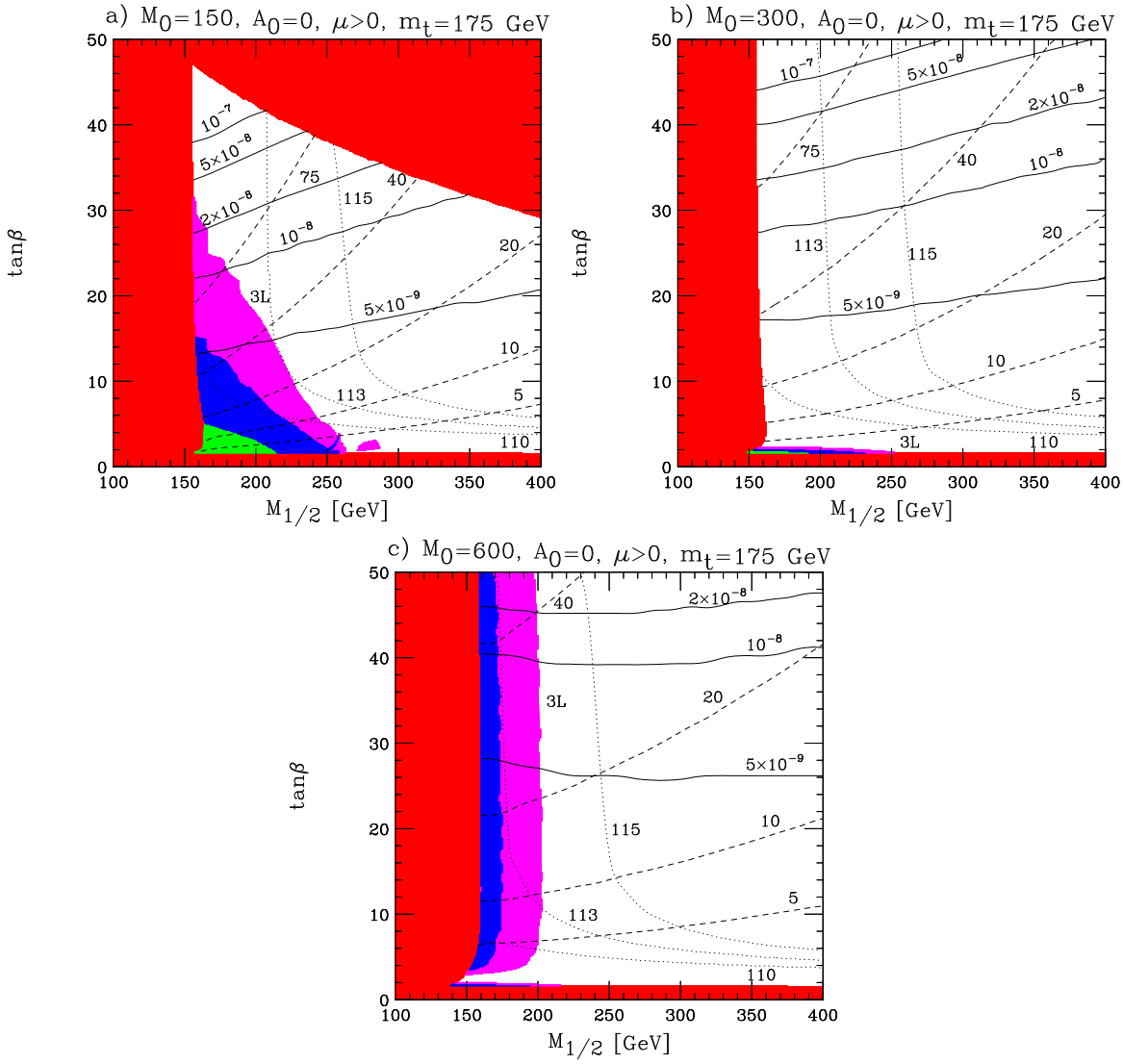

Figure 2: *Tevatron 5σ reach in the trilepton (3L) channel in the $M_{1/2} - \tan\beta$ plane for the mSUGRA scenario with a) $M_0 = 150$ GeV, b) $M_0 = 300$ GeV and c) $M_0 = 600$ GeV and $A_0 = 0$, $\mu > 0$ and $m_t = 175$ GeV. The shaded areas indicate integrated luminosities of $30fb^{-1}$ (magenta), $10fb^{-1}$ (blue) and $2fb^{-1}$ (green) and from top to bottom, respectively. Dashed contours represent the SUSY contribution to the muon anomalous magnetic moment (in units of 10^{-10}) and the dotted contours the Higgs boson mass. The solid contours indicate the prediction for $\mathcal{B}(B_s \to \mu^+\mu^-)$.*

Our next step is to present the simulation of the 3L events in the $M_{1/2} - \tan\beta$ plane for different values of M_0. Our results are depicted in Fig.2. For $M_0 = 150$ GeV, the 5σ reach of the Tevatron with $\mathcal{L} = 30fb^{-1}$ is bounded by $\tan\beta \lesssim 30$ and $M_{1/2} \lesssim 270$ GeV. In this region the Higgs mass is always below 114 GeV. With an integrated luminosity of $\mathcal{L} = 2fb^{-1}$, the Tevatron can observe the 3L events in a region with small $\tan\beta \leq 5$ and $M_{1/2} \leq 210$ GeV. In this region, the maximum Higgs mass is 109 GeV.

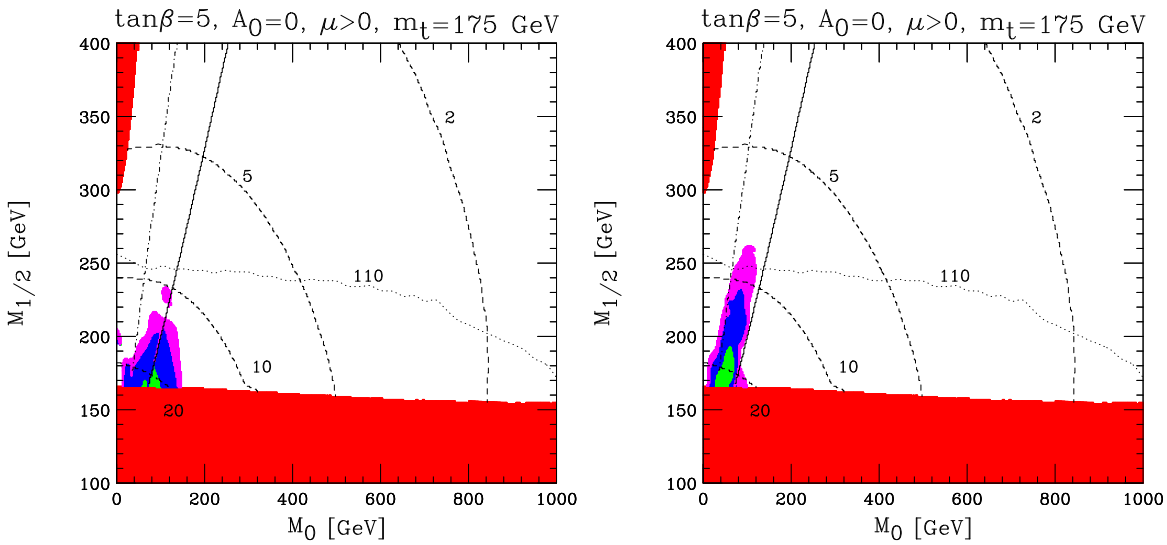

Figure 3: *Tevatron reach in the like sign dilepton channel (2L) (left) and and dilepton plus tau jet channel (2L1T) (right) for low* $\tan\beta = 5$ *and all the other parameters as in Fig.1. We do not observe these two modes at large* $\tan\beta = 50$*. Contours and shaded areas are as in Fig.1.*

As $\tan\beta$ increases, the stau mass decreases and the gaugino decays are mediated mostly by staus rather than sleptons. Gradually the 3L event rate is decreasing as we increase $\tan\beta$. When the 3L events are no longer observable, the branching ratio $\mathcal{B}(B_s \to \mu^+\mu^-)$ becomes significant and the decay $B_s \to \mu^+\mu^-$ has an observable rate of up to 30 events with $\mathcal{L} = 2fb^{-1}$. Moving to higher values of $M_0 = 300$ GeV (see Fig.2), the 3L events dissappear for the reason we have already explained when discussing Fig.1. However, a large portion of the parameter space with $\tan\beta \gtrsim 30$ is still accessible to $B_s \to \mu^+\mu^-$ searches. The parameter space with $\tan\beta$ values below 30 has to be covered by other searches, most probably Higgs searches (squarks and gluinos are too heavy to be directly discovered at Tevatron in the mSUGRA scenario [77].) The two cases $M_0 = 150\,\text{GeV}$ and $M_0 = 300\,\text{GeV}$ have to be considered respectively as the most "promising" and the "nightmare" benchmark scenarios for the Tevatron Run II. In order to complete the discussion on $M_{1/2} - \tan\beta$ plane we show in Fig. 2c the corresponding plot for $M_0 = 600$ GeV. This region is intermediate in search sensitivity and is bounded by $M_1/2 \lesssim 210$ GeV. It is largely independent of $\tan\beta$. A considerable amount of the remaining parameter space is covered by the search from $B_s \to \mu^+\mu^-$. We observe a considerable overlap between the two search regions for $\tan\beta \gtrsim 40$. For a complete analysis of the $B_s \to \mu^+\mu^-$ mode and other observables on $M_{1/2} - \tan\beta$ plane the reader is referred to Refs. [7, 22].

4.2 Other than 3L Channels

Apart from the trilepton (3L) analysis, we also study the modes with like sign dileptons (2L), dilepton plus tau-jet (2L1T), lepton plus two tau-jets (1L2T), three tau-jets (3T), like

sign lepton plus tau-jet (1L1T), and two like sign tau-jets (2T) in the final state. The idea is to identify alternative signatures in regions of the parameter space where the 3L signal is suppressed. For all these channels only the 2L and 2L1T survive our cuts and only in the small $\tan\beta \simeq 5$ region. The results are shown in Fig.3. Depending on the luminosity, we observe a 5σ reach at the Tevatron, in the mSUGRA regions:

$$(2L, \tan\beta = 5) \;:\; \begin{cases} M_0 \lesssim 120 \text{ GeV} \;,\; M_{1/2} \lesssim 175 \text{ GeV} \;,\; \mathcal{L} = 2fb^{-1}\,, \\ M_0 \lesssim 150 \text{ GeV} \;,\; M_{1/2} \lesssim 200 \text{ GeV} \;,\; \mathcal{L} = 10fb^{-1}\,, \\ M_0 \lesssim 160 \text{ GeV} \;,\; M_{1/2} \lesssim 230 \text{ GeV} \;,\; \mathcal{L} = 30fb^{-1}\,, \end{cases}$$

$$(2L1T, \tan\beta = 5) \;:\; \begin{cases} 40 \lesssim M_0 \lesssim 80 \text{ GeV} \;,\; M_{1/2} \lesssim 180 \text{ GeV} \;,\; \mathcal{L} = 2fb^{-1}\,, \\ 50 \lesssim M_0 \lesssim 100 \text{ GeV} \;,\; M_{1/2} \lesssim 260 \text{ GeV} \;,\; \mathcal{L} = 10fb^{-1}\,, \\ M_0 \lesssim 120\text{GeV} \;,\; M_{1/2} \lesssim 230 \text{ GeV} \;,\; \mathcal{L} = 30fb^{-1}\,, \end{cases}$$

Comparing with the Region I of the 3L signal, we see that an observation of 2L or/and 2L1T will pin down the parameters $M_0 - M_{1/2}$. In the $M_{1/2} - \tan\beta$ plane and for the optimistic benchmark $M_0 = 150\,\text{GeV}$, 2L events are only observable with $\mathcal{L} = 10(30)fb^{-1}$ for $M_{1/2} \lesssim 190, \tan\beta \lesssim 3$ ($M_{1/2} \lesssim 220, \tan\beta \lesssim 6$).

The search reach we obtain for signatures involving more than one hadronic tau are worse than those obtained previously [69]. The main reason for this is that we started from the leading-order Drell-Yan production processes with additional jets generated by the parton-shower algorithm for W and Z production, whereas [69] started from the W/Z+jets process. The study in [69] was also at the parton-level rather than using fast detector simulation. This means we have a much larger background from W/Z with fake taus. This agrees with the results of [53] where the signals with at least two electrons/muons gave the largest reach. It should also be noted the we took no account of the problems of triggering on the multi-hadronic tau final states which will make the situation even worse.

5 Conclusions

We have presented two complementary observables to study the parameter space of minimal supergravity at Run-II of the Fermilab Tevatron: the production of charginos or neutralinos decaying into trilepton (or other than trilepton) final states and the branching ratio of the rare decay $B_s \to \mu^+\mu^-$. The simulation of the trilepton events has been improved over previous results in various respects. In particular next-to-leading QCD corrections have been incorporated where available and the full momentum and spin correlations between production and decay of the supersymmetric particles have been taken into account. We have also presented modified cuts. With these enhancements we find the Tevatron reach for trilepton events increased. The two studied observables reveal very useful complementary information on the mSUGRA parameter space, covering the regions of small and large $\tan\beta$, respectively. Our results can be read directly from the Figs.1,2. For example, for $M_0 = 150\,\text{GeV}$, $A_0 = 0$ and $\mu > 0$ we find that a Run-IIb with 30 fb^{-1} will probe values of

$M_{1/2}$ in the range

$$M_{1/2} \quad \lesssim \quad 250\,\mathrm{GeV} \;-\; 70\,\mathrm{GeV} \times \frac{\tan\beta}{23},$$

which decreases with $\tan\beta$. On the contrary, if the Tevatron can measure $\mathcal{B}(B_s \to \mu^+\mu^-)$ down to 10^{-8} (which requires less than 30 fb^{-1} of integrated luminosity), this will probe the region with $\tan\beta > 32$ and the range

$$M_{1/2} \quad \lesssim \quad 19\,\mathrm{GeV} \times \tan\beta \;-\; 260\,\mathrm{GeV}$$

for the chosen values of M_0, A_0 and μ. Similar results can be drawn for other choices of the parameter M_0.

This work should be considered as a first attempt of relating "direct" SUSY searches such as the 3L events with an "indirect" rare B-decay, such as $B_s \to \mu^+\mu^-$ at the Tevatron.

Acknowledgments

We would like to thank M. Krämer and T. Plehn for providing the code used in [68] for next-to-leading order electroweak gaugino production. We would like to thank F. Krüger, J. Urban for illuminating discussions on the $B_s \to \mu^+\mu^-$ calculation. We also like to thank K. Matchev for his valuable comments on the trilepton analysis. A.D. would like to thank T. Kamon for discussions on the Tevatron 3L events, P. Slavich and S. Heinemeyer for useful discussions on the updates of the Higgs boson mass calculations. Preliminary results of this analysis have been presented by U.N. and A.D. at the Fermilab Users' meeting and SUSY02 conference, respectively. A.D. would like to acknowledge financial support from the Network RTN European Program HPRN-CT-2000-00148 "Physics Across the Present Energy Frontier: Probing the Origin of Mass". P.R. would like to thank PPARC for financial support.

References

[1] H. P. Nilles, Phys. Lett. B **115** (1982) 193; Nucl. Phys. B **217** (1983) 366; A. H. Chamseddine, R. Arnowitt and P. Nath, Phys. Rev. Lett. **49** (1982) 970; R. Barbieri, S. Ferrara and C. A. Savoy, Phys. Lett. B **119** (1982) 343; L. Hall, J. Lykken and S. Weinberg, Phys. Rev. D **27** (1983) 2359;

[2] S. K. Soni and H. A. Weldon, Phys. Lett. B **126** (1983) 215.

[3] E. Cremmer, B. Julia, J. Scherk, P. van Nieuwenhuizen, S. Ferrara and L. Girardello, Phys. Lett. B **79**, 231 (1978); E. Cremmer, B. Julia, J. Scherk, S. Ferrara, L. Girardello and P. van Nieuwenhuizen, Nucl. Phys. B **147**, 105 (1979).

[4] L. Girardello and M. T. Grisaru, Nucl. Phys. B **194** (1982) 65.

[5] H. P. Nilles, Phys. Rept. **110** (1984) 1.

[6] L. E. Ibanez and G. G. Ross, Phys. Lett. B **110** (1982) 215.

[7] A. Dedes, H. K. Dreiner and U. Nierste, Phys. Rev. Lett. **87**, 251804 (2001) [arXiv:hep-ph/0108037].

[8] D. A. Dicus, S. Nandi and X. Tata, Phys. Lett. B **129** (1983) 451 [Erratum-ibid. B **145** (1984) 448].

[9] H. Baer and X. Tata, Phys. Lett. B **155** (1985) 278.

[10] H. Baer, K. Hagiwara and X. Tata, Phys. Rev. Lett. **57** (1986) 294.

[11] H. Baer, K. Hagiwara and X. Tata, Phys. Rev. D **35** (1987) 1598.

[12] K. T. Matchev and D. M. Pierce, Phys. Lett. B **467** (1999) 225 [arXiv:hep-ph/9907505].

[13] K. T. Matchev and D. M. Pierce, Phys. Rev. D **60** (1999) 075004 [arXiv:hep-ph/9904282].

[14] G. Buchalla and A. J. Buras, Nucl. Phys. B **412**, 106 (1994) [hep-ph/9308272]; M. Misiak and J. Urban, Phys. Lett. B **451**, 161 (1999) [hep-ph/9901278].

[15] C. Bernard, Nucl. Phys. Proc. Suppl. **94**, 159 (2001) [hep-lat/0011064].

[16] *CKM fitter* group, `http://www.slac.stanford.edu/~laplace/ckmfitter/ckm_wellcome.html`

[17] W. Adam *et al.* [DELPHI Collaboration], Z. Phys. C **72**, 207 (1996).

[18] F. Abe *et al.* [CDF Collaboration], Phys. Rev. D **57**, 3811 (1998).

[19] The bound on $\mathcal{B}(B \to \tau^+\tau^-)$ from LEP I is a byproduct of the search for $B^- \to \tau^-\bar{\nu}$ pointed out in: Y. Grossman, Z. Ligeti and E. Nardi, Phys. Rev. D **55**, 2768 (1997) [arXiv:hep-ph/9607473]. This bound can be improved with the existing LEP data. We would like to thank M. Kobel and N. Wermes for discussions on this matter.

[20] T. Bergfeld *et al.* [CLEO Collaboration], Phys. Rev. D **62**, 091102 (2000) [arXiv:hep-ex/0007042].

[21] K. Anikeev *et al.*, arXiv:hep-ph/0201071.

[22] R. Arnowitt, B. Dutta, T. Kamon and M. Tanaka, arXiv:hep-ph/0203069.

[23] For a review on B physics at the LHC see for instance, P. Ball *et al.*, hep-ph/0003238.

[24] H. E. Logan and U. Nierste, Nucl. Phys. B **586**, 39 (2000) [hep-ph/0004139].

[25] C. S. Huang, W. Liao, Q. S. Yan and S. H. Zhu, Phys. Rev. D **63**, 114021 (2001) [Erratum-ibid. D **64**, 059902 (2001)] [arXiv:hep-ph/0006250]; P. H. Chankowski and L. Slawianowska, Phys. Rev. D **63**, 054012 (2001) [hep-ph/0008046].

[26] K. S. Babu and C. Kolda, Phys. Rev. Lett. **84**, 228 (2000) [hep-ph/9909476]; G. Isidori and A. Retico, JHEP **0111** (2001) 001 [arXiv:hep-ph/0110121].

[27] C. Bobeth, T. Ewerth, F. Krüger and J. Urban, Phys. Rev. D **64**, 074014 (2001) [arXiv:hep-ph/0104284].

[28] C. Hamzaoui, M. Pospelov and M. Toharia, Phys. Rev. D **59**, 095005 (1999) [hep-ph/9807350].

[29] D. A. Demir, K. A. Olive and M. B. Voloshin, arXiv:hep-ph/0204119.

[30] H. N. Brown *et al.* [Muon g-2 Collaboration], Phys. Rev. Lett. **86**, 2227 (2001) [hep-ex/0102017];

[31] M. Knecht and A. Nyffeler, arXiv:hep-ph/0111058. M. Knecht, A. Nyffeler, M. Perrottet and E. De Rafael, Phys. Rev. Lett. **88**, 071802 (2002) [arXiv:hep-ph/0111059]. The bound quoted in the text is taken from S. Narison, Phys. Lett. B **513**, 53 (2001) [Erratum-ibid. B **526**, 414 (2002)] [arXiv:hep-ph/0103199].

[32] S. w. Baek, P. Ko and W. Y. Song, arXiv:hep-ph/0205259.

[33] L. J. Hall, R. Rattazzi and U. Sarid, Phys. Rev. D **50** (1994) 7048 [arXiv:hep-ph/9306309]; M. Carena, D. Garcia, U. Nierste and C. E. Wagner, Nucl. Phys. B **577** (2000) 88 [arXiv:hep-ph/9912516].

[34] C. Bobeth, A. J. Buras, F. Kruger and J. Urban, Nucl. Phys. B **630**, 87 (2002) [arXiv:hep-ph/0112305].

[35] V. D. Barger, T. Gottschalk, D. V. Nanopoulos and R. J. Phillips, Phys. Rev. D **16** (1977) 3177.

[36] V. D. Barger and R. J. Phillips, Phys. Rev. D **30** (1984) 1890.

[37] A. H. Chamseddine, P. Nath and R. Arnowitt, Phys. Lett. B **129** (1983) 445 [Erratum-ibid. B **132** (1983) 467].

[38] P. Nath and R. Arnowitt, Mod. Phys. Lett. A **2** (1987) 331.

[39] H. Baer and X. Tata, Phys. Rev. D **47** (1993) 2739.

[40] H. Baer, C. h. Chen, F. Paige and X. Tata, Phys. Rev. D **50** (1994) 4508 [arXiv:hep-ph/9404212].

[41] H. K. Dreiner, M. Guchait and D. P. Roy, Phys. Rev. D **49** (1994) 3270 [arXiv:hep-ph/9310291].

[42] T. Kamon, J. L. Lopez, P. McIntyre and J. T. White, Phys. Rev. D **50** (1994) 5676 [arXiv:hep-ph/9406248].

[43] H. Baer, C. h. Chen, C. Kao and X. Tata, Phys. Rev. D **52** (1995) 1565 [arXiv:hep-ph/9504234].

[44] S. Mrenna, G. L. Kane, G. D. Kribs and J. D. Wells, Phys. Rev. D **53** (1996) 1168 [arXiv:hep-ph/9505245].

[45] H. Baer, C. H. Chen, R. Munroe, F. E. Paige and X. Tata, Phys. Rev. D **51** (1995) 1046 [arXiv:hep-ph/9408265].

[46] H. Baer, J. F. Gunion, C. Kao and H. Pois, Phys. Rev. D **51** (1995) 2159 [arXiv:hep-ph/9406374].

[47] J. L. Lopez, D. V. Nanopoulos, X. Wang and A. Zichichi, Phys. Rev. D **52** (1995) 142 [arXiv:hep-ph/9412346].

[48] H. Baer, C. h. Chen, M. Drees, F. Paige and X. Tata, Phys. Rev. Lett. **79** (1997) 986 [arXiv:hep-ph/9704457].

[49] H. Baer, C. h. Chen, M. Drees, F. Paige and X. Tata, Phys. Rev. D **58** (1998) 075008 [arXiv:hep-ph/9802441].

[50] V. D. Barger, C. Kao and T. j. Li, Phys. Lett. B **433** (1998) 328 [arXiv:hep-ph/9804451].

[51] V. D. Barger and C. Kao, Phys. Rev. D **60** (1999) 115015 [arXiv:hep-ph/9811489].

[52] H. Baer, C. h. Chen, M. Drees, F. Paige and X. Tata, Phys. Rev. D **59** (1999) 055014 [arXiv:hep-ph/9809223].

[53] J. D. Lykken and K. T. Matchev, Phys. Rev. D **61** (2000) 015001 [arXiv:hep-ph/9903238].

[54] M. Guchait and D. P. Roy, Phys. Lett. B **535** (2002) 243 [arXiv:hep-ph/0205015].

[55] H. Baer, M. Drees, F. Paige, P. Quintana and X. Tata, Phys. Rev. D **61** (2000) 095007 [arXiv:hep-ph/9906233].

[56] H. Baer, F. E. Paige, S. D. Protopopescu and X. Tata, arXiv:hep-ph/0001086.

[57] T. Sjostrand, Comput. Phys. Commun. **82** (1994) 74; S. Mrenna, Comput. Phys. Commun. **101** (1997) 232 [arXiv:hep-ph/9609360].

[58] A. Pukhov *et al.*, arXiv:hep-ph/9908288.

[59] G. Corcella *et al.*, JHEP **0101** (2001) 010 [arXiv:hep-ph/0011363]; G. Corcella *et al.*, arXiv:hep-ph/0201201; S. Moretti, K. Odagiri, P. Richardson, M. H. Seymour and B. R. Webber, JHEP **0204** (2002) 028 [arXiv:hep-ph/0204123].

[60] P. Richardson, JHEP **0111** (2001) 029 [arXiv:hep-ph/0110108].

[61] S. Jadach, Z. Was, R. Decker and J. H. Kühn, Comput. Phys. Commun. **76** (1993) 361.

[62] PGS detector simulation package **http://www.physics.rutgers.edu∼jconway/soft/pgs/pgs.htm**

[63] J. M. Campbell and R. K. Ellis, Phys. Rev. D **60** (1999) 113006 [arXiv:hep-ph/9905386].

[64] Talk given by K. Matchev at the conference *Higgs and Supersymmetry*, Gainesville, USA, March 7-11,1999.

[65] G. Corcella and M. H. Seymour, Nucl. Phys. B **565** (2000) 227 [arXiv:hep-ph/9908388].

[66] J. Campbell and R. K. Ellis, arXiv:hep-ph/0202176.

[67] R. Bonciani, S. Catani, M. L. Mangano and P. Nason, Nucl. Phys. B **529** (1998) 424 [arXiv:hep-ph/9801375].

[68] W. Beenakker, M. Klasen, M. Krämer, T. Plehn, M. Spira and P. M. Zerwas, Phys. Rev. Lett. **83** (1999) 3780 [arXiv:hep-ph/9906298].

[69] M. Guchait and D. P. Roy, arXiv:hep-ph/0109096.

[70] S. P. Martin and P. Ramond, Phys. Rev. D **48**, 5365 (1993) [arXiv:hep-ph/9306314].

[71] For the Higgs spectrum we use the code `FeynHiggs v1.2` in M. Frank, S. Heinemeyer, W. Hollik and G. Weiglein, arXiv:hep-ph/0202166 and references therein. The Higgs boson mass contours presented in the figures is slightly different than in [7] due to this update. The two loop bottom Yukawa corrections to the Higgs mass have been recently calculated in A. Brignole, G. Degrassi, P. Slavich and F. Zwirner, arXiv:hep-ph/0206101 . These corrections are negligible for our choice of the sign of the Higgsino mixing parameter.

[72] S. Heinemeyer and G. Weiglein, arXiv:hep-ph/0102117.

[73] [LEP Higgs Working Group Collaboration], "Searches for the neutral Higgs bosons of the MSSM: Preliminary combined results using LEP data collected at energies up to 209-GeV," arXiv:hep-ex/0107030. The result quoted here is preliminary.

[74] T. Moroi, Phys. Rev. D **53**, 6565 (1996) [Erratum-ibid. D **56**, 4424 (1996)] [arXiv:hep-ph/9512396].

[75] M. Carena *et al.*, arXiv:hep-ph/0010338.

[76] A. Djouadi, M. Drees and J. L. Kneur, JHEP **0108**, 055 (2001) [arXiv:hep-ph/0107316].

[77] S. Abel *et al.* [SUGRA Working Group Collaboration], arXiv:hep-ph/0003154.